Design, synthesis and biological evaluation of inhibitors of cathepsin K on dedifferentiated chondrocytes

Xiao-Yu Yuan, Zhongyuan Ren, Yuqing Wu, Carole Bougault, Leyre Brizuela, David Magne, Rene Ren, Saïda Mebarek

Design, synthesis and biological evaluation of inhibitors of cathepsin K on dedifferentiated chondrocytes

Xiao-Yu Yuan[1,3], Zhongyuan Ren[1], Yuqing Wu[1], Carole Bougault[2], Leyre Brizuela[2], David Magne[2], René Buchet[2] and Saida Mebarek[2*]

[1]State Key Laboratory of Supramolecular Structure and Materials, Jilin University, Changchun, 130012, China.

[2]Univ. Lyon, Univ. Claude Bernard Lyon 1, CNRS UMR 5246, ICBMS, F-69622, Lyon, France

[3]College of Food Science and Technology, Henan Agricultural University, Zhengzhou, 450002, China.

Corresponding author

Dr. Saida Mebarek

Université Lyon 1, ICMBS UMR CNRS5246

Batiment Raulin

43 Boulevard du 11 Novembre 1918

69622 Villeurbanne Cedex France

Email: saida.mebarek@univ-lyon1.fr

ABSTRACT:

Selective proteinase inhibitors have demonstrated utility in the investigation of cartilage degeneration mechanisms and may have clinical use in the management of osteoarthritis. The cysteine protease cathepsin K (CatK) is an attractive target for arthritis therapy. Here we report the synthesis of two cathepsin K inhibitors (CKIs): racemic azanitrile derivatives **CKI-E and CKI-F**, which have better inhibition properties on CatK than the commercial inhibitor odanacatib (ODN). Their IC_{50} values and inhibition constants (K_i) have been determined *in vitro.* Inhibitors demonstrate differential selectivity for CatK over cathepsin B, L and S *in vitro*, with K_i amounting to 1.14 and 7.21 nM respectively. We analyzed the effect of these racemic inhibitors on viability in different cell types. The human osteoblast-like cell line MG63, MOVAS cells (a murine vascular smooth muscle cell line) or murine primary chondrocytes, were treated either with CKI-E or with CKI-F, which were not toxic at doses of up to 5 µM. Primary chondrocytes subjected to several passages were used as a model of phenotypic loss of articular chondrocytes, occurring in osteoarthritic cartilage. The efficiency of CKIs regarding CatK inhibition and their specificity over other proteases were validated in primary chondrocytes subjected to several passages. Racemic CKI-E and CKI-F at 0.1 and 1 µM significantly inhibited CatK activity in dedifferentiated chondrocytes, even better than the commercial CatK inhibitor ODN. The enzymatic activity of other proteases such as matrix metalloproteinases or aggrecanases were not affected. Taken together, these findings support the possibility to design CatK inhibitors for preventing cartilage degradation in different pathologies.

Keywords: Azanitrile • cathepsin K inhibitors • chondrocyte • dedifferentiation • osteoarthritis

Abbreviations: CatK: cathepsin K, CKI: cathepsin K inhibitor, ODN: odanacatib, OA: Osteoarthritis

1. INTRODUCTION

Osteoarthritis (OA) is a very common age-related disease, affecting approximately 15% of the global population (1). Due to the demographic trends and ageing, OA is expected to affect more people in the forthcoming years (2). OA is a degenerative joint disorder characterized by irreparable destruction of the articular cartilage. Engineered cartilage has great potential in joint regeneration and reconstruction. A common cell source is chondrocytes, which are the sole cell type in articular cartilage. Its use is however restricted since autologous chondrocyte availability is limited in patients. Various *in vitro* cell expansion methods have been adopted to increase cell numbers before transplantation, but dedifferentiation of chondrocytes during this process remains an important challenge (3-6). Dedifferentiation evidences include cell shape change and decreased expression of cartilaginous matrix components such as collagens type II and type IX, as well as aggrecan (the major proteoglycan in the extracellular matrix) (3-6). Several experimental approaches are being developed to overcome the pitfalls of dedifferentiation (7). For instance, culturing chondrocytes on three-dimensional scaffold and/or adding cartilage growth factors may delay the dedifferentiation or favor the redifferentiation (8, 9). Of note, a knockdown of cathepsin K (CatK) has been shown to maintains the phenotype in expanded chondrocytes (10), indicating possible applications of CatK inhibition in tissue engineering and regenerative medicine.

CatK belongs to the family of papain-like cysteine peptidases (11). It is one of the main enzymes involved in bone resorption. Indeed, inhibition of CatK may serve as drug therapy to prevent osteoclast-related diseases (12, 13). Whereas the activity of most other cathepsins is restricted to the lysosomal compartment, CatK works extracellularly, preferentially under acidic pH conditions. At the molecular level, CatK is unique due to its ability to cleave the triple helix of collagen molecules at multiple locations. This activity is unparalleled among human collagenases (14). CatK has been demonstrated to be secreted by chondrocytes in OA patients and participates to the breakdown of cartilage collagen as well as proteoglycan

networks (15). A decrease in pH from 7 to 5.5 in the OA cartilage favors cysteine cathepsins over metalloproteinases (MMPs) as the major matrix degrading proteases in OA, at least in the later stages of the disease (15). The implication of CatK in OA cartilage degradation was demonstrated in mice, guinea pig, canine and rabbit models, and further confirmed by a chondroprotective effect of CatK inhibitors (CKIs) in OA pathology (16-18). Increased CatK expression and activation in human OA cartilage and synovial tissues were reported (12), indicating a possible effect of CatK on the pathogenesis of OA(12).

Many low molecular weight CKIs have been synthesized and tested for their specificity and ability to inhibit bone resorption (12, 13). Inhibitors that have emerged in recent years were designed to minimize unfavorable side effects, especially by synthesizing other classes of electrophiles like ketones and nitriles, capable of trapping the nucleophilic cysteine in a covalent yet reversible fashion (19-26). Several cathepsin inhibitors have previously fallen by the wayside. Novartis dropped its balicatib in 2006 because of dermatological adverse events (27, 28), and GlaxoSmithKline abandoned its relacatib in 2007, possibly because of off-target toxicity (29). Phase III clinical trials for odanacatib (ODN) (30-32) were stopped in 2016 by Merck, due to stroke risk (33). Among the cathepsin inhibitors that reached phase II trials, MIV-701 (34) was dedicated to the treatment of bone and cartilage related disorders in humans, such as OA, while ONO-5334 was evaluated for osteoporosis treatment in humans (35). Alternate CKIs, especially to prevent cartilage degradation in OA are needed, since only very few were tested to prevent cartilage degradation. In this report, we described the synthesis of two racemic CKIs, CKI-E and CKI-F, whose structures derived from previous CKIs (19), to improve inhibition properties against CatK. We compared their effects with those of the commercial inhibitor ODN. Inhibition parameters and selectivity over other cathepsins were assessed *in vitro*. Cell viability was tested in different cell types. Moreover, primary chondrocytes were dedifferentiated during several passages to mimic the phenotype

change of chondrocytes in OA cartilage. Dedifferentiated chondrocytes served to validate the efficiency of CKIs regarding CatK inhibition and their specificity over other proteases. In agreement with the literature (10), passages induced chondrocyte dedifferentiation with a loss of chondrogenic matrix production and an increase in CatK activity. We evaluated the ability of racemic CKI-E and racemic CKI-F to prevent collagen digestion by CatK in chondrocytes subjected to 0, 1, 2 and 3 passages. We aimed to provide a proof-of-concept of the potential of CKI treatment for preventing cartilage degradation during OA.

2. MATERIALS AND METHODS

2.1 Chemicals and reagents

Thin layer chromatography was performed on aluminum sheets from Branch of Qingdao Haiyang Chemical Co., Ltd. Preparative column chromatography was performed on silica gel 60, 54-74 μm. ^{1}H NMR (500 MHz) and ^{13}C NMR (126 MHz) spectra were recorded on a Bruker Avance 500 spectrometer. ESI-MS spectra were recorded on a Bruker HCT mass spectrometer. (4-(Methylsulfonyl) phenyl)boronic acid was bought from Alfa Aesar China (Tianjin Co., Ltd.); LDA (lithium diisopropylamide) was obtained from Shanghai Darui Finechemical Co., Ltd.; 1-iodo-2-methylpropane and THF (tetrahydrofuran) were bought from J&K Scientific Ltd.; 1,2-dimethylhydrazine dihydrochloride was obtained from TCI Co., Ltd.; cyanogen bromide was bought from ACROS Co., Ltd.

2.2 Synthesis routes for CKI-E and -F.

Compound **1′** (Figure 1) was obtained by using the same synthesis procedure as described before (19, 36), therefore its synthesis will not be described in detail.

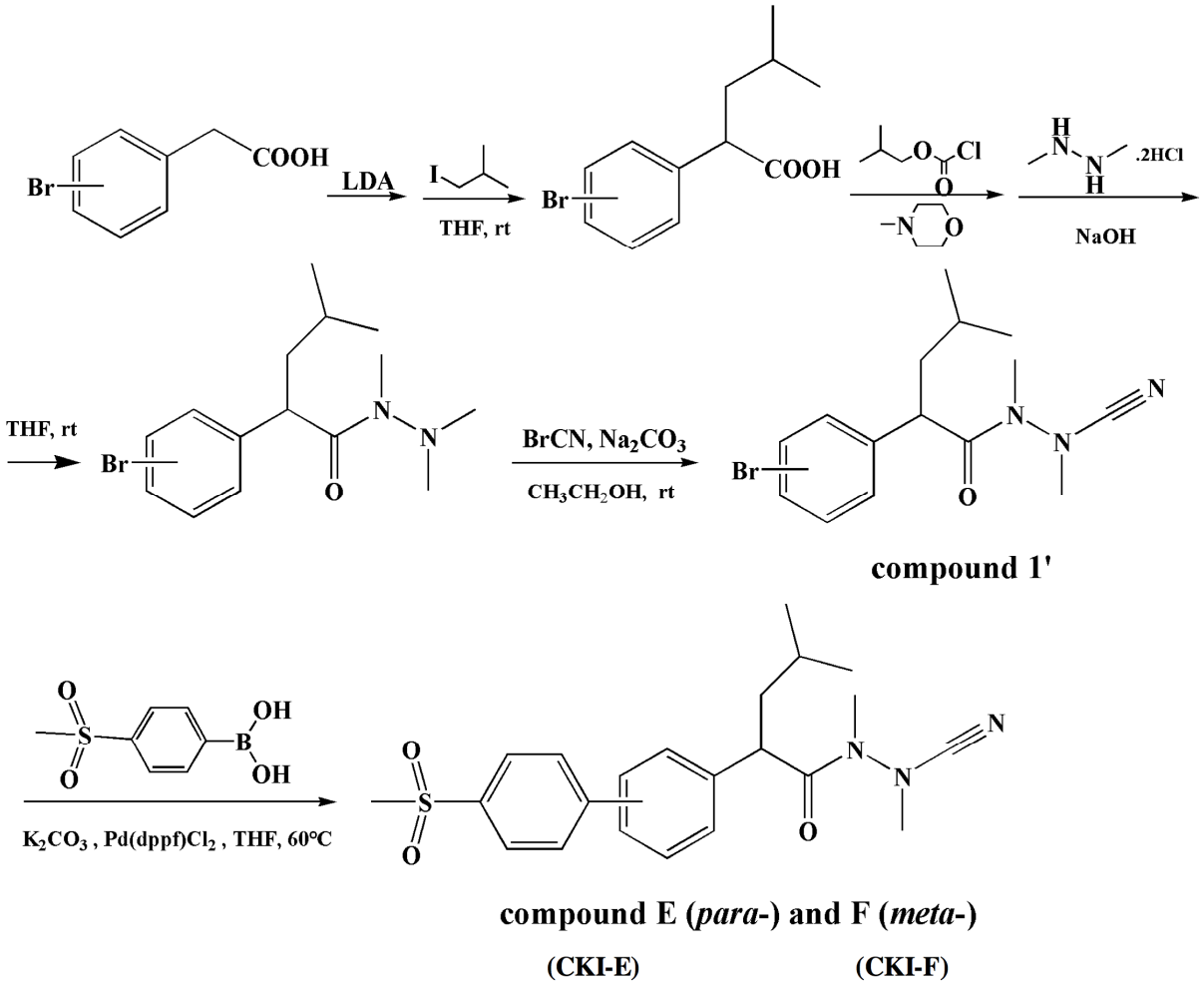

Figure 1. Synthesis route for compounds CKI-E and CKI-F.

2.2.1 N'-cyano-N,N',4-trimethyl-2-(4'-(methylsulfonyl)-[1,1'-biphenyl]-4-yl)pentanehydrazide (racemic CKI-E)

100 mL round-bottomed Schlenk flask equipped with a magnetic stir bar was charged with 0.34 g compound **1′** (bromide as para position) (1 mmol), 0.24 g (4-(methylsulfonyl) phenyl) boronic acid (1.2 mmol), 0.058 g tetrakis(triphenylphosphine) palladium (0.05 mmol), 2 mL of 1 M aqueous solution of Na_2CO_3, and 30 mL of tetrahydrofurane (37) (Figure 1). The mixture was degassed using five cycles of vacuum/nitrogen back-fill firstly, and then it was heated up to 70 °C and kept there for 2.5 h with vigorous stirring. In following, the mixture

was cooled down to room temperature, and the solvent was removed under reduced pressure. The residue was then suspended in H_2O (10 mL) and ethyl acetate (30 mL), the organic layer was separated while the aqueous layer was extracted with ethyl acetate (3×15 mL). The combined organic phases were washed with brine (2×15 mL), and then dried with Na_2SO_4 and evaporated to obtain the crude product of N'-cyano-N,N',4-trimethyl-2-(4'-(methylsulfonyl)-[1,1'-biphenyl]-4-yl)pentanehydrazide, which was then purified by column chromatography on silica gel using ethyl acetate / petroleum ether (1:1) as eluent. HPLC chromatogram indicated that CKI-E was highly pure (around 95%) as estimated by negligible intensities of contaminant compounds (HPLC: t = 2.5min).

^{1}H NMR (500 MHz, $CDCl_3$): δ 8.03 (d, *J* = 8.2 Hz, 2H), δ 7.78 (d, *J* = 8.3 Hz, 2H), δ 7.61 (d, *J* = 8.2 Hz, 2H), δ 7.46 (dd, *J* = 22.0, 9.8 Hz, 2H), δ 4.26 (t, *J* = 7.2 Hz, 1H), δ 3.21 (s, 4H), δ 3.12 (s, 3H), δ 2.62 (s, 3H), δ 2.09 - 1.98 (m, 1H), δ 1.66 (dt, *J* = 29.6, 11.4 Hz, 1H), δ 1.52 (dt, *J* = 13.7, 7.0 Hz, 1H), δ 1.01-0.94 (m, 6H),

^{13}C NMR (126 MHz, $CDCl_3$): δ 174.48 (s), δ 145.85 (s), δ 140.32 (s), δ 139.28 (s), δ 137.99 (s), δ 128.74 (s), δ 127.91 (d, *J*=18.6 Hz), δ 113.91 (s), δ 45.81 (s), δ 44.61 (s), δ 43.58 (s), δ 40.59 (s), δ 30.64 (s), δ 25.67 (s), δ 22.71 (s), δ 22.40 (s).

MS (ESI) m/z: 414.1841$[M + H]^+$, 827.3567 $[2M + H]^+$.

2.2.2 N'-cyano-N,N',4-trimethyl-2-(4'-(methylsulfonyl)-[1,1'-biphenyl]-3-yl)pentanehydrazide (racemic CKI-F)

CKI-F (Figure 1) was produced by using the similar procedures as those for CKI-E except compound **1′** (bromide as meta position). The crude product of N'-cyano-N,N',4-trimethyl-2-(4'-(methylsulfonyl)-[1,1'-biphenyl]-4-yl)pentanehydrazide was obtained and purified similarly by column chromatography on silica gel using tetrahydrofuran / petroleum ether

(1:2) as eluent . HPLC chromatogram indicated that CKI-F was highly pure (about 95%) as estimated by negligible intensities of contaminant compounds (HPLC: t = 2.7min).

^{1}H NMR (500 MHz, $CDCl_3$): δ 8.04 (d, *J* = 8.1 Hz, 2H), δ 7.80 (dd, *J* = 18.9, 8.1 Hz, 1H), δ 7.58 - 7.51(m, 2H), δ 7.47 (dd, *J* = 15.1, 7.4 Hz, 1H), δ 4.30 (dt, *J* = 14.8, 7.2 Hz, 1H), δ 3.20 (s, 3H), δ 3.12 (s, 4H), δ 2.59 (s, 2H), δ 2.15 - 1.81 (m, 2H), δ 1.50 (ddd, *J* = 22.6, 14.0, 7.2 Hz, 1H), δ 0.97 (dd, *J* = 10.9, 4.3 Hz, 6H)

^{13}C NMR (126 MHz, $CDCl_3$): δ 174.50 (s), δ 146.02 (s), δ 140.75 (s), δ 139.87 (s), δ 139.49 (s), δ 129.69 (s), δ 128.54 – 127.67 (m), 126.61 (d, *J* = 8.7 Hz), δ 126.29 (s), δ 46.19 (s), δ 44.64 (s), δ 43.73 (s), δ 40.57 (s), δ 30.67 (s), δ 25.74 (s), δ 22.64 (s), δ 22.47 (s).

MS (ESI) m/z: 414.1839 $[M + H]^+$, 827.3571 $[2M + H]^+$.

2.3 *In vitro* performed inhibition assays

Inhibition assays were performed using commercial recombinant cathepsins to determine the concentrations of half maximal inhibition (IC_{50}) of CKI-E and CKI-F. The experimental conditions for the inhibition assays of human CatK (Merck 219461, His-Tag, Human, recombinant, *E.coli*. Germany), cathepsin L (CatL) (Merck 219402, Human Liver, Germany), cathepsin S (CatS) (Merck 219343, Human, recombinant, *E. coli*, Germany) and cathepsin B (CatB) (Merck 219362, human liver, Germany) were described before (21, 36). We have previously determined the Michaelis constant (K_m) for CatK, L, S and B to be 18.06 ± 0.22 μM, 3.525 ± 0.405 μM, 102.2 ± 1.52 μM and 157.5 ± 2.5 μM, respectively (21). IC_{50} values determined in this work, K_m and the concentration of substrate [S] were used to calculate the inhibition constant of the inhibitors (K_i), by using the following equation:

$$K_i = \frac{IC_{50}}{\left(1+\frac{[S]}{K_m}\right)} \qquad (1)$$

2.4 Cell culture

2.4.1 Ethics statements

All experiments were carried out according to the guidelines laid down by the French Ministère de l'Agriculture (n° 87-848) and the E.U. Council Directive for the Care and Use of Laboratory Animals of November 24th, 1986 (86/609/EEC). Animal experiments were performed under the authorization n°69-266-0501 (INSA-Lyon, DDPP-SV, Direction Départementale de la Protection des Populations - Services Vétérinaires du Rhône). MLC (n°692661241), AG (n°69266332) and COS (n°69266257) hold special licenses to experiment on living vertebrates issued by the French Ministry of Agriculture and Veterinary Service Department. The experiments were realized on euthanized animals by dislocation of cervical vertebra, which did not require surgery and were not painful.

2.4.2 Cell models

Two commercial cell lines were used: the mouse vascular smooth muscle cell line MOVAS (ATCC® CRL-2797™) and the human osteoblast-like cell line MG-63 (ATCC® CRL-1427™). In addition, primary chondrocytes were isolated as described previously (38) from the epiphyseal cartilage of the humerus and femur of 5-6 day-old mice (SWISS strain). All three cell models were cultured in growing medium containing DMEM (Dulbecco's Modified Eagle Medium) with 10% (v:v) Fetal Bovine Serum (FBS), 100 U mL^{-1} penicillin and 100 µg mL^{-1} streptomycin. When primary cells reached confluency, they were harvested using trypsin-EDTA (Sigma Aldrich, Lyon, FR) and split in two sets. One set was sub-cultured, that is to say passaged, and the other set was collected for further analysis. This procedure was repeated so that primary chondrocytes were analyzed at 4 time points: passages 0, 1, 2 and 3 (P0, P1, P2, P3). All cells were incubated in a humidified atmosphere consisting of 95 % air and 5 % CO_2 at 37 °C.

2.5 Cell viability assay

For cell viability assay, the cells were plated in 12-well plates (Corning inc, 60000 cells/well for chondrocytes, 100 000 cells/well for cell lines) and were cultured in DMEM, containing 10% (v:v) FBS, 100 $U.mL^{-1}$ penicillin and 100 $\mu g.mL^{-1}$ streptomycin without (control) or with CKIs at different concentrations until confluence. Their viability was measured using the MTT (3-(4, 5-dimethylthiazol-2-yl)-2,5-diphenyltetrazolium bromide) colorimetric assay methods (Roche Diagnostics, Meylan, France) as described previously (39). MTT labeling reagent (0.125 mg mL^{-1} final concentration) was added to each well and the cells were further incubated for 4 h. Culture supernatant was replaced by 1 mL of solubilization solution (dimethyl sulfoxide). Cell viability was directly related to absorbance measured at 570 nm using a Tecan Infinite M200 (Salzburg, Austria) micro-titre plate reader. Results were normalized relative to their respective controls (0.1% DMSO (v:v) without CKI), taken as

100% of viability. For each inhibitor/cell combination, three distinct sample pools were analyzed in a triplicate manner (n = 9).

2.6 Zymography of matrix metalloproteinases and CatK in culture medium and cell lysates

Zymography of matrix metalloproteinases (MMPs) and CatK were performed accordingly to literature (40, 41). Briefly, extracellular medium (containing secreted MMPs) and primary chondrocyte lysate (containing intracellular CatK) were collected at 4 time points (P0, P1, P2, P3), in extraction buffer (pH 7.5) containing 20 mM Tris-HCl, 5 mM ethylene glycol tetraacetic acid (EGTA), 150 mM NaCl, 10 mM NaF, 20 mM ß-glycerol phosphate (ß-GP), 1 mM sodium orthovanadate, 1% (v:v) Triton X-100 and 0.1% (v:v) Tween 20. Equal amounts of protein were resolved either by 12% SDS-polyacrylamide gels containing 2 $mg.mL^{-1}$ gelatin for revealing enzymatic activity of CatK, or by 8% (v:v) SDS-polyacrylamide gels containing 1.2 $mg.mL^{-1}$ gelatin, for revealing enzymatic activity of (MMPs). Gels were washed in renaturing buffer containing 65 mM Tris, (pH=7.38), 20% (v:v) glycerol for 45 min, twice. An acidic buffer (pH 6.0) containing 100 mM sodium phosphate buffer, 1 mM EDTA and 2 mM dithiothreitol, was used to reveal the activity of CatK selectively. To reveal the activity of MMPs, gels were incubated in buffer (pH 7.4) containing 50 mM Tris, 20 mM NaCl and 5 mM $CaCl_2$. After 30 min, these activity buffers were exchanged to fresh ones containing 0.1% DMSO (v:v) without (control) or with CKI for 24 h of incubation at 37 °C. Finally, gels were rinsed twice with deionized water before incubation for 1 h in a Coomassie staining solution (2.5 mg mL^{-1} Coomassie blue), 45% (v:v) methanol, 10% (v:v) acetic acid) for labeling the gelatin. This step was followed by a bath in distaining solution (30% (v:v) methanol, 10% (v:v) acetic acid). The gels were scanned using a Canon scanner. Disappearance of gelatin from gels, as evidenced by lack of coloration, indicated activity of CatK or MMPs.

2.7 Fluorescence measurement for quantitative determination of CatK activity

Chondrocyte lysates were obtained by adding the same extraction buffer that was used for zymography. CatK activity was detected at the cellular level according to the method of Dolbeare and Smith (42) by means of the substrate Z-Gly-Pro-Arg-4-methoxy-β-naphthylamide (Z-GPR-4MβNA, 1 mg mL^{-1}). The hydrolysis of Z-GPR-4-MβNA by CatK liberated 4-methoxy-β-naphthylamide (4MβNA). To quantify the CatK activity, 4MβNA was precipitated and detected by 5-nitro-salicylaldehyde at 10 µM final concentration (Sigma-Aldrich), which is an accumulating fluorescent product. The CatK activity was normalized to the protein concentration [C] according to the equation:

$$\text{CatK activity} = \frac{F_{sc} - F_{si}}{[C]} \quad (2)$$

where F_{sc} was the fluorescence of the control (containing the substrate and DMSO 0.1% (v:v)), while F_{si} was the fluorescence of the sample containing the substrate with or without CKIs. Fluorescence was determined with a F-4500 fluorescence spectrophotometer (Thermo Scientific, Germany) at least three times for each condition, with excitation and emission wavelength of 488 and 525 nm (fluorescein setting), respectively. Protein concentration was measured using Braford assay (43).

2.8 Alcian Blue staining

Chondrocyte phenotype was evaluated by measuring the extracellular sulfated glycosaminoglycans (sGAG) deposition using Alcian blue staining. Briefly, the culture medium was removed from culture plates, cells were gently washed once with phosphate-buffered saline (PBS, 137 mM sodium chloride, 10 mM phosphate, 2.7 mM potassium chloride; pH 7.4) and then fixed in 4% (v:v) of formaldehyde solution for 30 min at room temperature (42). After fixation, cells were rinsed with PBS and stained for 30 min with 1% Alcian blue (m:v) solution prepared in 0.1 N HCl. Finally, staining was dissolved with 33%

isopropanol in GnCl (4.0 mol/L) and the absorbance was determined by a microplate reader (Thermo Scientific) at 595 nm. The blue staining indicated the presence of acidic sGAG, markers of chondrocyte phenotype.

2.9 Data analyses and statistical analyses

All graphs and statistical analyses were performed using GraphPad Prism software. For each graphic analysis, at least three independent experiments were performed. Non-parametric Mann-Whitney test was used to analyze data. Results were expressed as mean ± standard error of the mean (SEM) or standard error (SD), as indicated. Results were considered significant when $p < 0.05$ (*), highly significant when $p < 0.01$ (**), and extremely significant when $p < 0.001$ (***).

3. RESULTS

3.1 Synthesis routes for compounds CKI-E and CKI-F.

We have previously reported the synthesis of several CKIs (19, 36). We reasoned that the removal of amide linkage in CKI-8 and CKI-13 (Figure 2) would improve the selectivity due to elimination of hydrogen bonds involving the amide group.

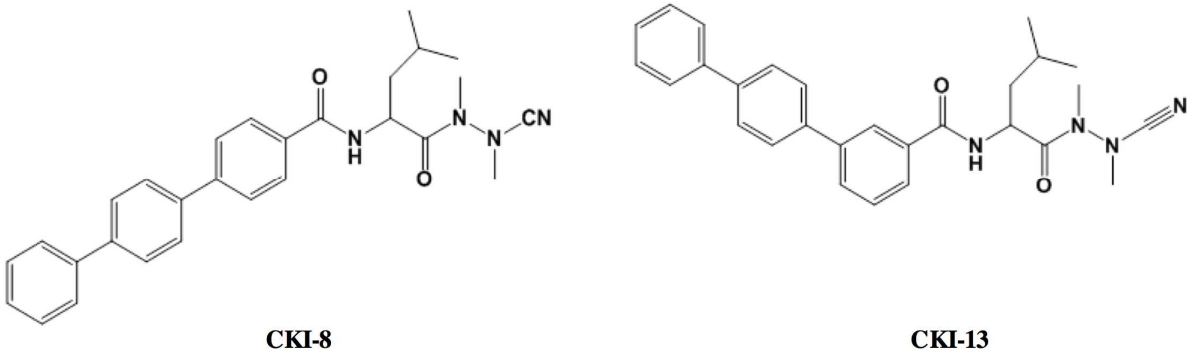

CKI-8 **CKI-13**

Figure 2: Structures of CKI-8 and CKI-13 (36).

The compound **1**' was produced by using the same procedures as formerly reported（19, 36). Racemic compounds CKI-E and CKI-F were synthesized as shown in Figure 1. Both products' structures were validated by $^{13}C/^{1}H$ NMR–and MS. In addition, our HPLC results indicated that CKI-E and CKI-F compounds were highly pure (about 95% of purity).

3.2 *In vitro* affinity and selectivity of racemic CKI- E and racemic CKI-F for CatK

The concentrations of half maximal inhibition (IC_{50}) were determined *in vitro* determining CatK activity in the presence of increasing doses of CKI-E (Figure 3A) or CKI-F (Figure 4A). In parallel, IC_{50} were assessed for CatL, CatS and CatB to evaluate the selectivity of CKI-E (Figure 3B, 3C, 3D) and CKI-F (Figure 4B, 4C, 4D).

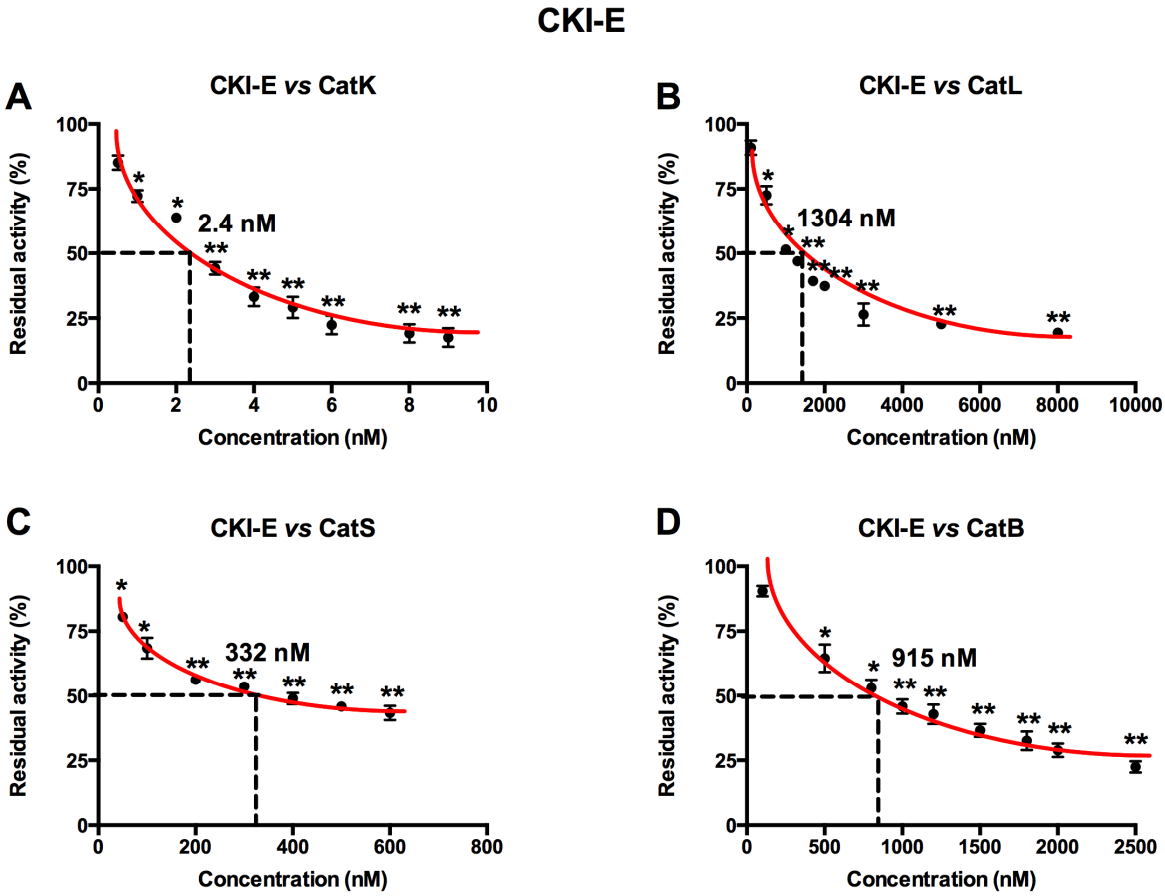

Figure 3. Determination of IC_{50} values of racemic compound CKI-E against CatK (A), Cat L (B), Cat S (C) and Cat B (D). Experiences were realized at least 4 times independently. Results are represented as mean ± SD.

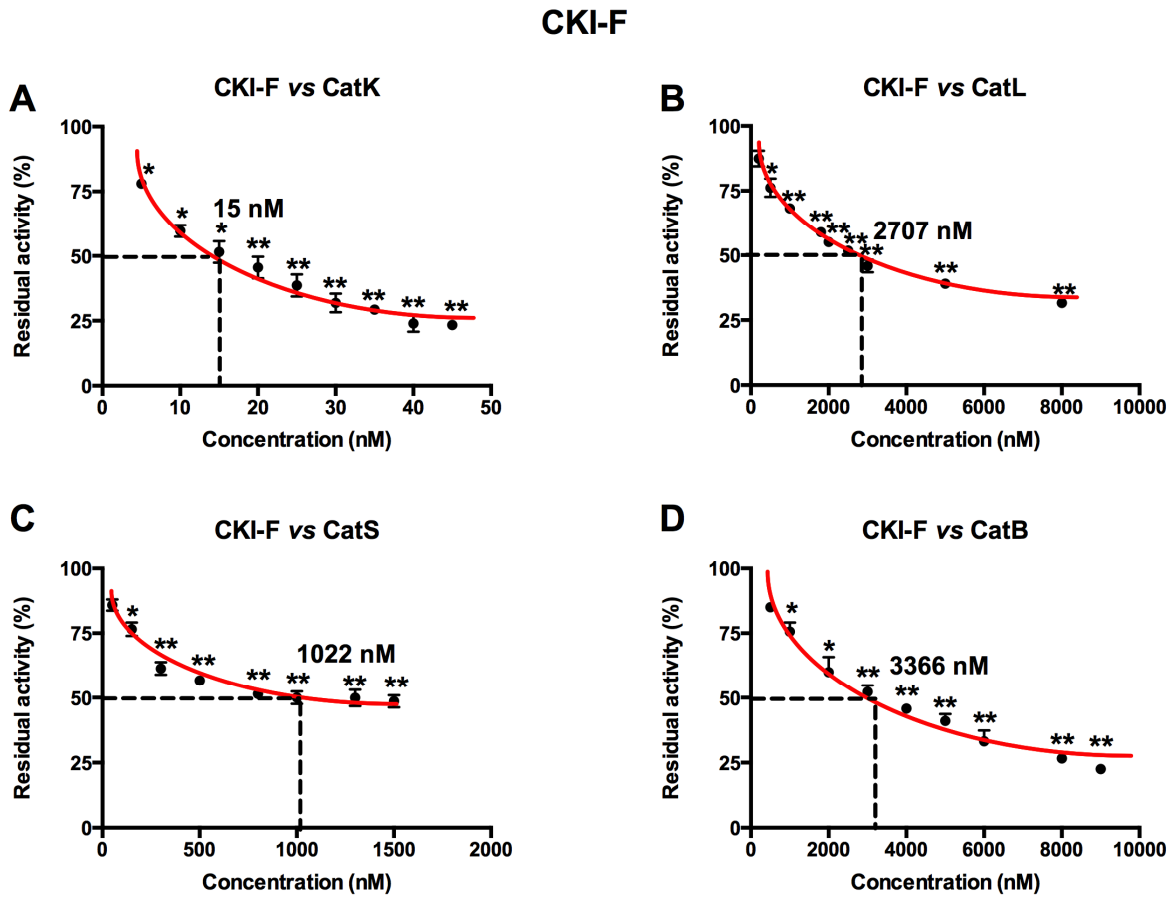

Figure 4. Determination of IC_{50} values of racemic compound CKI-F against CatK (A), Cat L (B), Cat S (C) and Cat B (D). Experiences were realized at least 4 times independently. Results are represented as mean ± SD.

The low IC_{50} of 2.4 nM for CKI-E and of 15 nM for CKI-F indicated that both compounds were strong inhibitors of human CatK. These values, by using equation (1), allowed to calculate inhibition constants (K_i), which amounted to 1.1 nM for CKI-E and to 7.2 nM for CKI-F, respectively (Table 1). Moreover, both CKI-E and CKI-F showed a substantial

selectivity for CatK over CatL, S and B. In the case of CKI-E, the K_i for other cathepsins were at least 170-fold higher than for CatK, and 50-fold higher in the case of CKI-F (Table 1). According to this enzymatic *in vitro* analysis, CKI-E seemed superior to CKI-F due to its higher affinity for CatK and due to its better selectivity for CatK over the other three enzymes, especially over CatL. Both CatK and L are endopeptidases with high sequence homology (60% identity, 76% similarity), which made it very difficult to be inhibited selectively. We suggest that the isobutyl group of CKI-E and CKI-F were not adequately packed into the S2 pocket formed by Leu69, Met70, Ala135, Met161, Asp162, Gly164 and Ala214 in CatL, explaining that CKI-E and CKI-F had higher affinity for CatK as compared to that for CatL. Indeed, the bad orientation of CKI-E and CKI-F in the S2 pocket might be attributed to the fact that cathepsin L preferred large aromatic group as the bi(hetero)aryl group.

Table 1. K_i constants of two racemic aza-peptide nitrile inhibitors CKI-E and CKI-F for different cathepsins: CatK, CatL, CatS and CatB.

Compounds	K_i (nM) of enzymes			
	CatK	CatL	CatS	CatB
CKI-E	1.14±0.03	195±25	239±12	909±102
CKI-F	7.21±0.16	406±54	735±37	3345±374

The only difference between the isomeric inhibitors CKI-E and CKI-F is the occurrence of the meta- and para- biphenyl substructure, respectively, which changed the orientation of the P3 substituent relative to entire molecule. This dissimilarity can distinctly affect the orientation of the compounds within the active site of the target protease.

3.3 Effects of inhibitors on the viability of MG63 and MOVAS cell lines and primary chondrocytes

The cytotoxicity of the two racemic compounds CKI-E and CKI-F was tested on three distinct cell types: human osteoblast-like cell line MG63 (Figure 5A), murine vascular smooth muscle cell line MOVAS (Figure 5B) and murine primary chondrocytes (Figure 5C). MTT viability assays were performed after 3 days incubation with or without inhibitors (control). The addition of DMSO up to 0.1% (v:v), which was the solvent used to solubilize the inhibitors, did not affect cell viability. Racemic CKI-E and CKI-F were not toxic in the concentration range from 1 nM to 5 µM on the different type of cells tested (Figure 5).

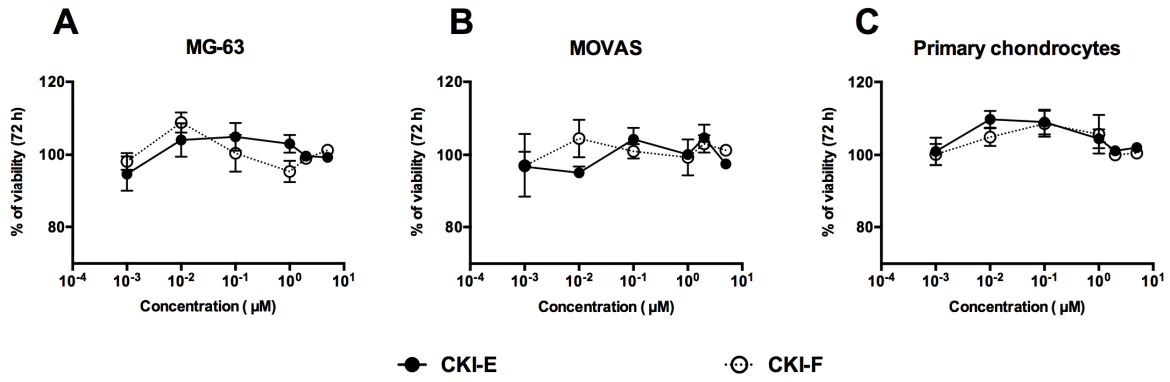

Figure 5. Effects of inhibitors on the viability of MG63, MOVAS line cells and primary chondrocytes. MG-63 (A) and MOVAS cell line (B) or murine primary chondrocytes (C) were treated with increasing concentrations of CKI-E and CKI-F. Three independent experiments were performed in triplicate Results are represented as mean ± SEM.

3.4 Up-regulated CatK activity in dedifferentiated chondrocytes

As expected, we observed that the morphology of chondrocytes changed with increasing number of passages (Figure 6A). After P2 and P3, cells exhibited a fibroblastic elongated morphology, as opposed to the characteristic paving pattern of well-differentiated chondrocytes (P0). In addition, we observed by Alcian blue staining that, as soon as-P1, the

deposition of glycosaminoglycans in the extracellular matrix dropped drastically (Figure 6B). Because a high content in proteoglycans is a feature of cartilaginous matrix, this analysis confirmed chondrocyte dedifferentiation in our model. Using fluorogenic substrate assays and zymography, we measured CatK activity from chondrocytes at different passages (Figure 6C, 6D). We observed that relative activity of CatK rose from P0 to P1 and P2 and then slightly decreased after P3. Fluorometric assays showed an average increase in relative CatK activity of 5%, 40% and 20% after P1, P2 and P3 respectively, by comparison to P0 (Figure 6C). This finding was further confirmed by zymography as the activity follows the same profile, with a particularly sustained band at P2 (Figure 6D, asterisk). This result confirmed a gradual up-regulation of CatK activity in passaged chondrocytes, especially at P2.

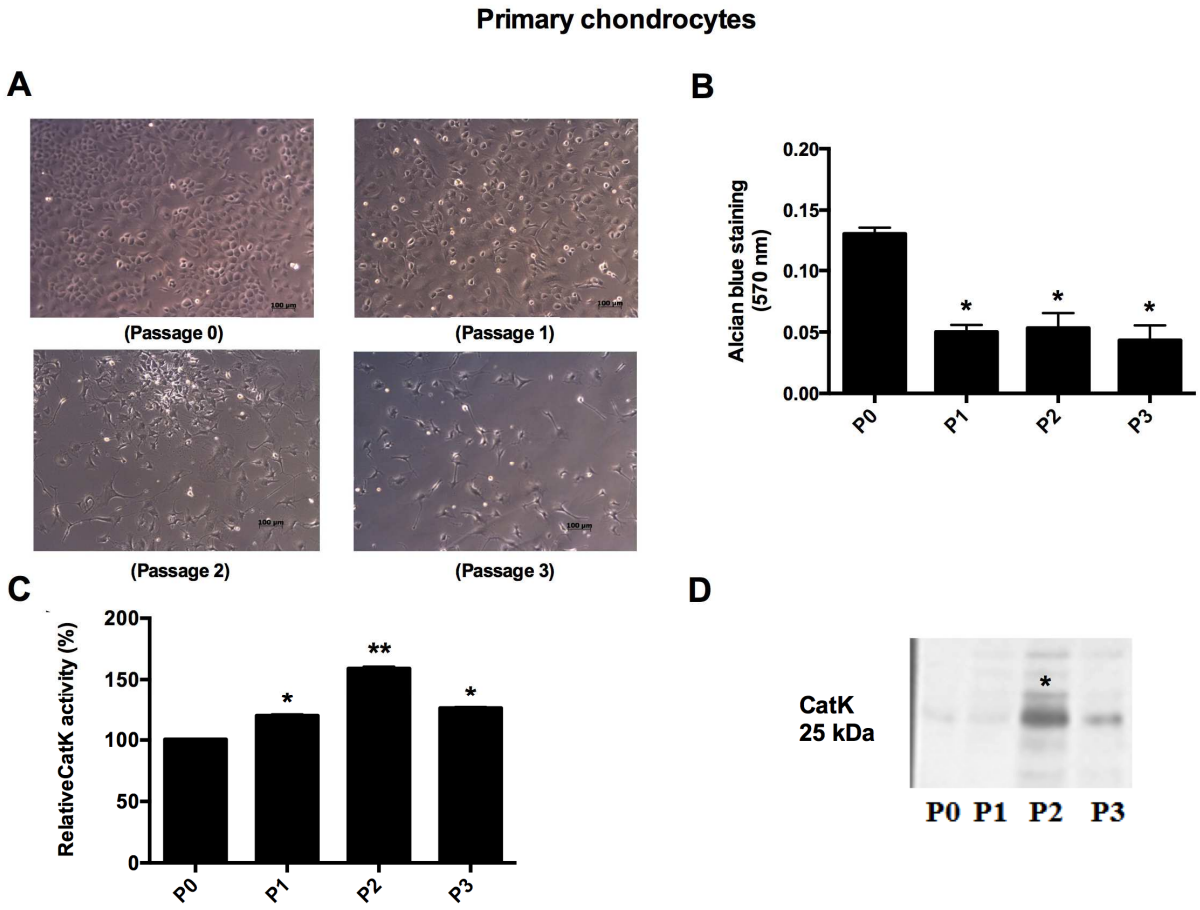

Figure 6. Characterization of isolated articular chondrocytes using monolayer passaging. Morphology of chondrocytes with increasing number of passages **(A).** Alcian blue

staining in primary chondrocytes after P0, P1, P2 or P3 **(B)**. Effect of primary chondrocyte passages on CatK activity measured by fluorescence assay **(C)** and by zymography **(D).** Three independent experiments were performed in triplicate. Results are represented as mean ± SEM. Non-parametric Mann-Whitney test was performed to evaluate significant differences. * p <0.05, **<0.01.

3.5 Effect of racemic CKI-E and racemic CKI-F inhibitors on CatK activity compared to ODN

We compared the effects of ODN, racemic CKI-E and racemic CKI-F on the activity of CatK in dedifferentiated primary murine chondrocytes at P2 as probed by fluorescence with Z-GPR-4MβNA as substrate (Figure 7A) and by zymography (Figure 7B). CKI-E, CKI-F and ODN at 0.1 and 1 µM inhibited significantly (p value <0.001) CatK activity in chondrocytes (Figure 7A). We detected an average reduction of 25-35% for CKI-E and 30-40% for CKI-F, while ODN induced a decrease of 19-30%. CKI-E and CKI-F inhibited CatK significantly better than ODN treatment. Furthermore, CKI-F was significantly more efficient than CKI-E to block CatK activity. This inhibition was confirmed by zymography, using gels pre-incubated with ODN, CKI-E and CKI-F at 1 µM (Figure 7B). Both CKI-E and CKI-F inhibitors were able to block the gelatinolytic activity of CatK from P2 chondrocytes, even better than ODN. The addition of 0.1% (v:v) DMSO used to solubilize the inhibitors did not affect the inhibition. At equal concentration, the efficiency of both CKI-E and CKI-F to block CatK activity seemed superior to that of ODN.

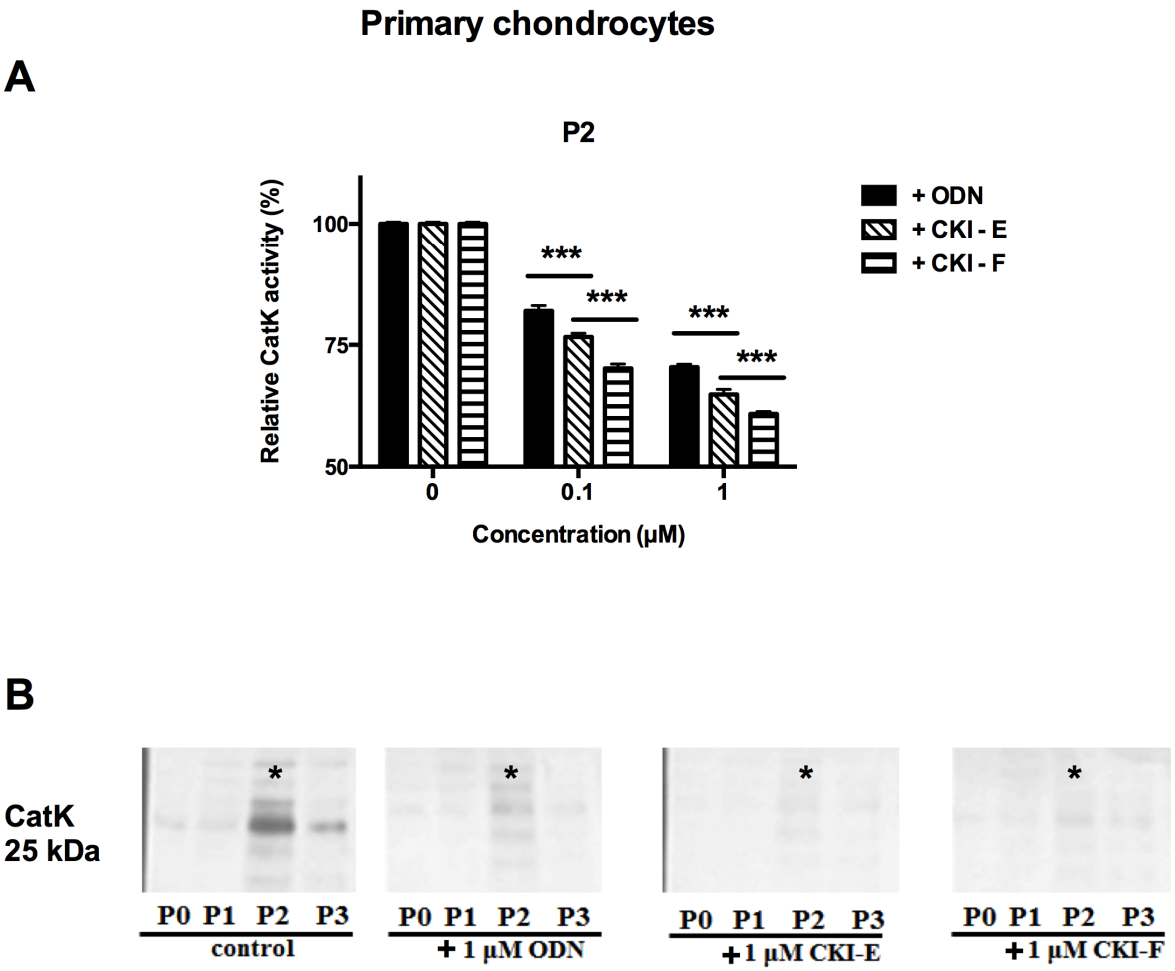

Figure 7. Effect of inhibitors on CatK activity in dedifferentiated chondrocytes (passage 2). (A) Effect of 0.1 and 1 µM ODN, CKI-E, CKI-F on CatK activity in chondrocytes after P2 probed by fluorescence assay. (**B)** Effect of ODN, CKI-E and CKI-F at 1 µM on CatK activity in primary chondrocytes after P0, P1, P2 and P3 as revealed by zymography. Three independent experiments were performed in triplicate. Control corresponded to CatK activity in chondrocytes without the presence of any inhibitors. Results are represented as mean ± SEM. Non-parametric Mann-Whitney test was performed to evaluate significant differences. * $p<0.05$, *** $p<0.001$.

3.6 Effect of inhibitors on other cartilage matrix proteases, such as aggrecanases and MMPs

Cultured chondrocyte dedifferentiation as well as OA chondrocyte degeneration are accompanied by an increase in matrix-degrading enzymes (44) such as aggrecanases or MMPs. We wondered if our inhibitors could affect these proteases (Figure 8). We previously observed by Alcian blue staining that the deposition of glycosaminoglycans in the extracellular matrix dropped drastically after passages (Figure 6B). Here, we demonstrated that addition of any of our CKIs at 1 µM did not affect glycosaminoglycans content in chondrocytes at P0, P1 and P2 (Figure 8A), indicating that these inhibitors did not prevent the aggregan loss, whether due to a decreased production or an increased degradation by aggrecanase activity. We also checked if racemic CKI-E and racemic CKI-F can affect MMP-2 and -9 activity by zymography. As expected, we observed that P2 induced the activity of MMP-2 and -9 in dedifferentiated chondrocytes, in comparison with P0 (Figure 8B, control). Pre-incubation of the gels with ODN, CKI-E and CKI-F at 1 µM, did not affect the MMP gelatinolytic activity of P0 or P2 chondrocytes (Figure 8B, ODN, CKI-E, CKI-F). Of note, the addition of 0.1% (v:v) DMSO used to solubilize the inhibitors did not affect the inhibition either. Therefore, neither aggrecanases nor MMP-2 and -9 protease activities were affected by ODN, CKI-E and CKI-F.

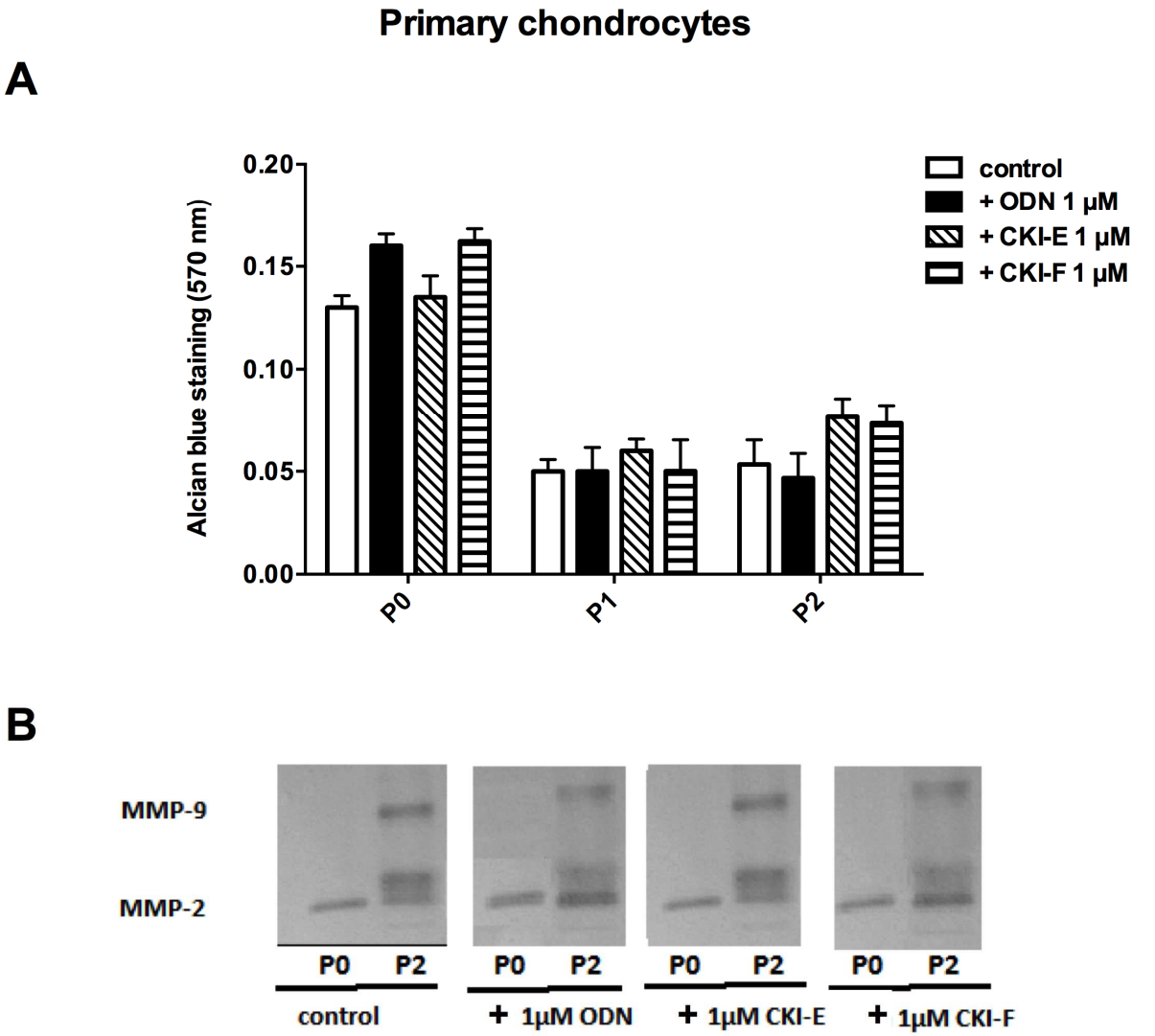

Figure 8. Effect of inhibitors on other cartilage matrix proteases, such as aggrecanases and MMPs. (A) Alcian blue staining in primary chondrocytes after P0, P1 and P2 in the presence or in the absence of CatK inhibitors at 1µM. Three independent experiments were performed in triplicate. Results are represented as mean ± SEM. Non-parametric Mann-Whitney test was performed to evaluate significant differences. * $p<0.05$, *** $p<0.001$. (**B)** Gelatinase activity (MMP-2 and 9) with or without CatK inhibitors at 1 µM was determined by zymography. Each experiment was realized in triplicate.

4. Discussion

From the first generation of inhibitors (19, 21, 22, 45), we synthetized two racemic azanitrile compounds CKI-E and CKI-F, which were found to be highly selective for CatK over B, L and S *in vitro*, with K_i amounting to 1.14 and 7.21 nM respectively. CKI-E and CKI-F showed no toxicity on three distinct cell types, up to 5 µM, which is three orders of magnitude greater than K_i. CKI-E and CKI-F at 0.1 and 1 µM significantly inhibited CatK activity in chondrocytes, even better than the commercial CatK inhibitor ODN. It was earlier suggested that the prevention of cartilage degradation by CatK inhibition may represent a valid strategy for pharmacological intervention in OA (18). The experimental evidence accumulated in this work supports the possibility to use CKIs for preventing cartilage degradation and the interest of the CKIs for engineered cartilage therapy and OA treatment.

A large network of proteases can orchestrate cartilage degradation in OA. This network includes not only CatK but also aggrecanases (46), responsible for aggregan degradation, and MMPs (47), affecting collagen degradation in degenerative cartilage diseases as OA. Targeting enzymes degrading cartilage has already been considered as a possible strategy to treat OA. Inhibitors of aggrecanases (47, 48), ADAMTS (49) and MMPs (50) indicated strong promises in preventing cartilage degradation. Among the gene-based methods already developed, only a few addressed cartilage matrix proteases. The optimization of the knock-down of MMP-3 and -13 by nanoparticles encoding shRNA has given promising results (51). Moreover, the inhibition of aggrecanase-1 and -2 expression by a lentiviral delivery system (52) or the knock-down of CatK in expanded chondrocytes (51) had similar valuable effects on phenotype maintenance. The expression of chondrocyte markers collagen II and aggrecan was increased and the modified cells formed a more homogenous matrix enriched in collagens and proteoglycans (51, 53). Combined therapy with CKIs and other inhibitor of proteases could be effective to treat degenerative cartilage diseases, especially OA.

5. Funding Statement

Yuqing Wu appreciates the financial support from the projects of NSFC (No. 21373101); Xiaoyu Yuan and Zhongyuan Ren appreciate the supports from National Student Fund Committee. The China-France cooperation project was funded by PHC Cai Yuanpei (Project N° 32065TD).

REFERENCES

1. Johnson VL, Hunter DJ. The epidemiology of osteoarthritis. Best Practice & Research in Clinical Rheumatology. 2014;28(1):5-15. doi: 10.1016/j.berh.2014.01.004. PubMed PMID: WOS:000337010300002.
2. Mueller MB, Tuan RS. Anabolic/Catabolic Balance in Pathogenesis of Osteoarthritis: Identifying Molecular Targets. Pm&R. 2011;3(6):S3-S11. doi: 10.1016/j.pmrj.2011.05.009. PubMed PMID: WOS:000305437800002.
3. Schulze-Tanzil G, Mobasheri A, de Souza P, John T, Shakibaei M. Loss of chondrogenic potential in dedifferentiated chondrocytes correlates with deficient Shc-Erk interaction and apoptosis. Osteoarthritis Cartilage. 2004;12(6):448-58. doi: 10.1016/j.joca.2004.02.007. PubMed PMID: 15135141.
4. Schulze-Tanzil G, de Souza P, Villegas Castrejon H, John T, Merker HJ, Scheid A, et al. Redifferentiation of dedifferentiated human chondrocytes in high-density cultures. Cell Tissue Res. 2002;308(3):371-9. Epub 2002/05/18. doi: 10.1007/s00441-002-0562-7. PubMed PMID: 12107430.
5. Cournil-Henrionnet C, Huselstein C, Wang Y, Galois L, Mainard D, Decot V, et al. Phenotypic analysis of cell surface markers and gene expression of human mesenchymal stem cells and chondrocytes during monolayer expansion. Biorheology. 2008;45(3-4):513-26. PubMed PMID: 18836250.
6. Zaucke F, Dinser R, Maurer P, Paulsson M. Cartilage oligomeric matrix protein (COMP) and collagen IX are sensitive markers for the differentiation state of articular primary chondrocytes. Biochem J. 2001;358(Pt 1):17-24. PubMed PMID: 11485547; PubMed Central PMCID: PMCPMC1222027.
7. Rai V, Dilisio MF, Dietz NE, Agrawal DK. Recent strategies in cartilage repair: A systemic review of the scaffold development and tissue engineering. J Biomed Mater Res A. 2017;105(8):2343-54. Epub 2017/05/10. doi: 10.1002/jbm.a.36087. PubMed PMID: 28387995.
8. Caron MM, Emans PJ, Coolsen MM, Voss L, Surtel DA, Cremers A, et al. Redifferentiation of dedifferentiated human articular chondrocytes: comparison of 2D and 3D cultures. Osteoarthritis Cartilage. 2012;20(10):1170-8. Epub 2012/07/10. doi: 10.1016/j.joca.2012.06.016. PubMed PMID: 22796508.
9. Claus S, Mayer N, Aubert-Foucher E, Chajra H, Perrier-Groult E, Lafont J, et al. Cartilage-characteristic matrix reconstruction by sequential addition of soluble factors during expansion of human articular chondrocytes and their cultivation in collagen sponges. Tissue Eng Part C Methods. 2012;18(2):104-12. Epub 2011/11/14. doi: 10.1089/ten.tec.2011.0259. PubMed PMID: 21933021.
10. Zhang Y, Li J, Zhu J, Zhou G, Zhang WJ, Cao Y, et al. Enhanced cartilage formation by inhibiting cathepsin K expression in chondrocytes expanded in vitro. Biomaterials. 2012;33(30):7394-404. Epub 2012/07/20. doi: 10.1016/j.biomaterials.2012.06.070. PubMed PMID: 22818652.
11. Novinec M, Lenarčič B. Cathepsin K: a unique collagenolytic cysteine peptidase. Biol Chem. 2013;394(9):1163-79. doi: 10.1515/hsz-2013-0134. PubMed PMID: 23629523.
12. Drake MT, Clarke BL, Oursler MJ, Khosla S. Cathepsin K Inhibitors for Osteoporosis: Biology, Potential Clinical Utility, and Lessons Learned. Endocr Rev. 2017;38(4):325-50. doi: 10.1210/er.2015-1114. PubMed PMID: 28651365; PubMed Central PMCID: PMCPMC5546879.
13. Lu J, Wang M, Wang Z, Fu Z, Lu A, Zhang G. Advances in the discovery of cathepsin K inhibitors on bone resorption. J Enzyme Inhib Med Chem. 2018;33(1):890-904. doi: 10.1080/14756366.2018.1465417. PubMed PMID: 29723068; PubMed Central PMCID: PMCPMC6010086.
14. Novinec M, Kovacic L, Lenarcic B, Baici A. Conformational flexibility and allosteric regulation of cathepsin K. Biochemical Journal. 2010;429:379-89. doi: 10.1042/bj20100337. PubMed PMID: WOS:000280085000016.

15. Konttinen YT, Mandelin J, Li TF, Salo J, Lassus J, Liljeström M, et al. Acidic cysteine endoproteinase cathepsin K in the degeneration of the superficial articular hyaline cartilage in osteoarthritis. Arthritis Rheum. 2002;46(4):953-60. PubMed PMID: 11953972.
16. Hayami T, Zhuo Y, Wesolowski GA, Pickarski M, Duong lT. Inhibition of cathepsin K reduces cartilage degeneration in the anterior cruciate ligament transection rabbit and murine models of osteoarthritis. Bone. 2012;50(6):1250-9. doi: 10.1016/j.bone.2012.03.025. PubMed PMID: 22484689.
17. McDougall JJ, Schuelert N, Bowyer J. Cathepsin K inhibition reduces CTXII levels and joint pain in the guinea pig model of spontaneous osteoarthritis. Osteoarthritis Cartilage. 2010;18(10):1355-7. doi: 10.1016/j.joca.2010.07.014. PubMed PMID: 20692355.
18. Connor JR, LePage C, Swift BA, Yamashita D, Bendele AM, Maul D, et al. Protective effects of a cathepsin K inhibitor, SB-553484, in the canine partial medial meniscectomy model of osteoarthritis. Osteoarthritis and Cartilage. 2009;17(9):1236-43. doi: 10.1016/j.joca.2009.03.015. PubMed PMID: WOS:000270118500017.
19. Ren Z-Y, Machuca-Gayet I, Domenget C, Buchet R, Wu Y, Jurdic P, et al. Azanitrile Cathepsin K Inhibitors: Effects on Cell Toxicity, Osteoblast-Induced Mineralization and Osteoclast-Mediated Bone Resorption. Plos One. 2015;10(7). doi: 10.1371/journal.pone.0132513. PubMed PMID: WOS:000358193100049.
20. Grabowskal U, Chambers TJ, Shiroo M. Recent developments in cathepsin K inhibitor design. Curr Opin Drug Discov Devel. 2005;8(5):619-30. PubMed PMID: 16159024.
21. Ren XF, Li HW, Fang X, Wu Y, Wang L, Zou S. Highly selective azadipeptide nitrile inhibitors for cathepsin K: design, synthesis and activity assays. Org Biomol Chem. 2013;11(7):1143-8. doi: 10.1039/c2ob26624e. PubMed PMID: 23299878.
22. Yang PY, Wang M, Li L, Wu H, He CY, Yao SQ. Design, synthesis and biological evaluation of potent azadipeptide nitrile inhibitors and activity-based probes as promising anti-Trypanosoma brucei agents. Chemistry. 2012;18(21):6528-41. Epub 2012/04/04. doi: 10.1002/chem.201103322. PubMed PMID: 22488888.
23. Frizler M, Lohr F, Furtmann N, Kläs J, Gütschow M. Structural optimization of azadipeptide nitriles strongly increases association rates and allows the development of selective cathepsin inhibitors. J Med Chem. 2011;54(1):396-400. doi: 10.1021/jm101272p. PubMed PMID: 21128614.
24. Löser R, Frizler M, Schilling K, Gütschow M. Azadipeptide nitriles: highly potent and proteolytically stable inhibitors of papain-like cysteine proteases. Angew Chem Int Ed Engl. 2008;47(23):4331-4. doi: 10.1002/anie.200705858. PubMed PMID: 18404765.
25. Schmitz J, Beckmann AM, Dudic A, Li T, Sellier R, Bartz U, et al. 3-Cyano-3-aza-β-amino Acid Derivatives as Inhibitors of Human Cysteine Cathepsins. ACS Med Chem Lett. 2014;5(10):1076-81. doi: 10.1021/ml500238q. PubMed PMID: 25313316; PubMed Central PMCID: PMCPMC4190633.
26. Frizler M, Lohr F, Lülsdorff M, Gütschow M. Facing the gem-dialkyl effect in enzyme inhibitor design: preparation of homocycloleucine-based azadipeptide nitriles. Chemistry. 2011;17(41):11419-23. Epub 2011/09/05. doi: 10.1002/chem.201101350. PubMed PMID: 21898616.
27. Jerome C, Missbach M, Gamse R. Balicatib, a cathepsin K inhibitor, stimulates periosteal bone formation in monkeys. Osteoporos Int. 2012;23(1):339-49. Epub 2011/03/05. doi: 10.1007/s00198-011-1593-2. PubMed PMID: 21380636.
28. Rünger TM, Adami S, Benhamou CL, Czerwiński E, Farrerons J, Kendler DL, et al. Morphea-like skin reactions in patients treated with the cathepsin K inhibitor balicatib. J Am Acad Dermatol. 2012;66(3):e89-96. Epub 2011/05/14. doi: 10.1016/j.jaad.2010.11.033. PubMed PMID: 21571394.
29. Kumar S, Dare L, Vasko-Moser JA, James IE, Blake SM, Rickard DJ, et al. A highly potent inhibitor of cathepsin K (relacatib) reduces biomarkers of bone resorption both in vitro and in an acute model of elevated bone turnover in vivo in monkeys. Bone. 2007;40(1):122-31. Epub 2006/09/07. doi: 10.1016/j.bone.2006.07.015. PubMed PMID: 16962401.
30. Bone HG, Dempster DW, Eisman JA, Greenspan SL, McClung MR, Nakamura T, et al. Odanacatib for the treatment of postmenopausal osteoporosis: development history and design and participant characteristics of LOFT, the Long-Term Odanacatib Fracture Trial. Osteoporos Int. 2014. doi: 10.1007/s00198-014-2944-6. PubMed PMID: 25432773.

31. Bone HG, McClung MR, Roux C, Recker RR, Eisman JA, Verbruggen N, et al. Odanacatib, a cathepsin-K inhibitor for osteoporosis: a two-year study in postmenopausal women with low bone density. J Bone Miner Res. 2010;25(5):937-47. doi: 10.1359/jbmr.091035. PubMed PMID: 19874198.
32. Stoch SA, Zajic S, Stone JA, Miller DL, van Bortel L, Lasseter KC, et al. Odanacatib, a selective cathepsin K inhibitor to treat osteoporosis: safety, tolerability, pharmacokinetics and pharmacodynamics--results from single oral dose studies in healthy volunteers. Br J Clin Pharmacol. 2013;75(5):1240-54. doi: 10.1111/j.1365-2125.2012.04471.x. PubMed PMID: 23013236; PubMed Central PMCID: PMCPMC3635595.
33. Mullard A. Merck &Co. drops osteoporosis drug odanacatib. Nat Rev Drug Discov. 2016;15(10):669. doi: 10.1038/nrd.2016.207. PubMed PMID: 27681784.
34. Lindström E, Rizoska B, Henderson I, Terelius Y, Jerling M, Edenius C, et al. Nonclinical and clinical pharmacological characterization of the potent and selective cathepsin K inhibitor MIV-711. J Transl Med. 2018;16(1):125. Epub 2018/05/09. doi: 10.1186/s12967-018-1497-4. PubMed PMID: 29743078; PubMed Central PMCID: PMCPMC5944028.
35. Tanaka M, Hashimoto Y, Hasegawa C, Deacon S, Eastell R. Antiresorptive effect of a cathepsin K inhibitor ONO-5334 and its relationship to BMD increase in a phase II trial for postmenopausal osteoporosis. BMC Musculoskelet Disord. 2017;18(1):267. Epub 2017/06/19. doi: 10.1186/s12891-017-1625-y. PubMed PMID: 28629344; PubMed Central PMCID: PMCPMC5477094.
36. Yuan XY, Fu DY, Ren XF, Fang X, Wang L, Zou S, et al. Highly selective aza-nitrile inhibitors for cathepsin K, structural optimization and molecular modeling. Org Biomol Chem. 2013;11(35):5847-52. doi: 10.1039/c3ob41165f. PubMed PMID: 23900712.
37. Kaupp G, Naimi-Jamal MR, Stepanenko V. Waste-free and facile solid-state protection of diamines, anthranilic acid, diols, and polyols with phenylboronic acid. Chemistry. 2003;9(17):4156-61. doi: 10.1002/chem.200304793. PubMed PMID: 12953200.
38. Gosset M, Berenbaum F, Thirion S, Jacques C. Primary culture and phenotyping of murine chondrocytes. Nat Protoc. 2008;3(8):1253-60. doi: 10.1038/nprot.2008.95. PubMed PMID: 18714293.
39. Mosmann T. Rapid colorimetric assay for cellular growth and survival: application to proliferation and cytotoxicity assays. J Immunol Methods. 1983;65(1-2):55-63. PubMed PMID: 6606682.
40. Toth M, Fridman R. Assessment of Gelatinases (MMP-2 and MMP-9 by Gelatin Zymography. Methods in molecular medicine. 2001;57:163-74. doi: 10.1385/1-59259-136-1:163. PubMed PMID: MEDLINE:21340898.
41. Li WA, Barry ZT, Cohen JD, Wilder CL, Deeds RJ, Keegan PM, et al. Detection of femtomole quantities of mature cathepsin K with zymography. Anal Biochem. 2010;401(1):91-8. doi: 10.1016/j.ab.2010.02.035. PubMed PMID: 20206119.
42. Dolbeare FA, Smith RE. Flow cytometric measurement of peptidases with use of 5-nitrosalicylaldehyde and 4-methoxy-beta-naphthylamine derivatives. Clin Chem. 1977;23(8):1485-91. PubMed PMID: 17486.
43. Bradford MM. A rapid and sensitive method for the quantitation of microgram quantities of protein utilizing the principle of protein-dye binding. Anal Biochem. 1976;72:248-54. doi: S0003269776699996 [pii]. PubMed PMID: 942051.
44. Ashraf S, Cha BH, Kim JS, Ahn J, Han I, Park H, et al. Regulation of senescence associated signaling mechanisms in chondrocytes for cartilage tissue regeneration. Osteoarthritis Cartilage. 2016;24(2):196-205. Epub 2015/07/16. doi: 10.1016/j.joca.2015.07.008. PubMed PMID: 26190795.
45. Ren ZY, Machuca-Gayet I, Domenget C, Buchet R, Wu Y, Jurdic P, et al. Azanitrile Cathepsin K Inhibitors: Effects on Cell Toxicity, Osteoblast-Induced Mineralization and Osteoclast-Mediated Bone Resorption. PLoS One. 2015;10(7):e0132513. doi: 10.1371/journal.pone.0132513. PubMed PMID: 26168340; PubMed Central PMCID: PMCPMC4500499.
46. Malemud CJ. Matrix Metalloproteinases and Synovial Joint Pathology. Prog Mol Biol Transl Sci. 2017;148:305-25. Epub 2017/05/04. doi: 10.1016/bs.pmbts.2017.03.003. PubMed PMID: 28662824.

47. Dancevic CM, McCulloch DR. Current and emerging therapeutic strategies for preventing inflammation and aggrecanase-mediated cartilage destruction in arthritis. Arthritis Res Ther. 2014;16(5):429. PubMed PMID: 25606593; PubMed Central PMCID: PMCPMC4289229.
48. El Bakali J, Gras-Masse H, Maingot L, Deprez B, Dumont J, Leroux F, et al. Inhibition of aggrecanases as a therapeutic strategy in osteoarthritis. Future Med Chem. 2014;6(12):1399-412. doi: 10.4155/fmc.14.84. PubMed PMID: 25329196.
49. Mead TJ, McCulloch DR, Ho JC, Du Y, Adams SM, Birk DE, et al. The metalloproteinase-proteoglycans ADAMTS7 and ADAMTS12 provide an innate, tendon-specific protective mechanism against heterotopic ossification. JCI Insight. 2018;3(7). Epub 2018/04/05. doi: 10.1172/jci.insight.92941. PubMed PMID: 29618652; PubMed Central PMCID: PMCPMC5928868.
50. Xie XW, Wan RZ, Liu ZP. Recent Research Advances in Selective Matrix Metalloproteinase-13 Inhibitors as Anti-Osteoarthritis Agents. ChemMedChem. 2017;12(15):1157-68. Epub 2017/07/19. doi: 10.1002/cmdc.201700349. PubMed PMID: 28722301.
51. Zhao J, Fan X, Zhang Q, Sun F, Li X, Xiong C, et al. Chitosan-plasmid DNA nanoparticles encoding small hairpin RNA targeting MMP-3 and -13 to inhibit the expression of dedifferentiation related genes in expanded chondrocytes. J Biomed Mater Res A. 2014;102(2):373-80. Epub 2013/05/14. doi: 10.1002/jbm.a.34711. PubMed PMID: 23520014.
52. Wang ZH, Yang ZQ, He XJ, Kamal BE, Xing Z. Lentivirus-mediated knockdown of aggrecanase-1 and -2 promotes chondrocyte-engineered cartilage formation in vitro. Biotechnol Bioeng. 2010;107(4):730-6. doi: 10.1002/bit.22862. PubMed PMID: 20632367.
53. Bourgoin SG, Zhao C. Autotaxin and lysophospholipids in rheumatoid arthritis. Curr Opin Investig Drugs. 2010;11(5):515-26. PubMed PMID: 20419597.

CKI-E and CKI-F, specific inhibitors of Cathepsin K, an attractive target for arthritis therapy

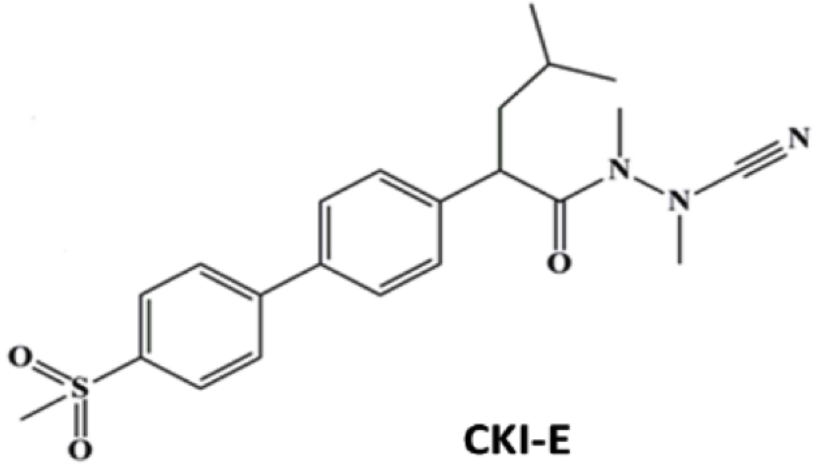

CKI-E

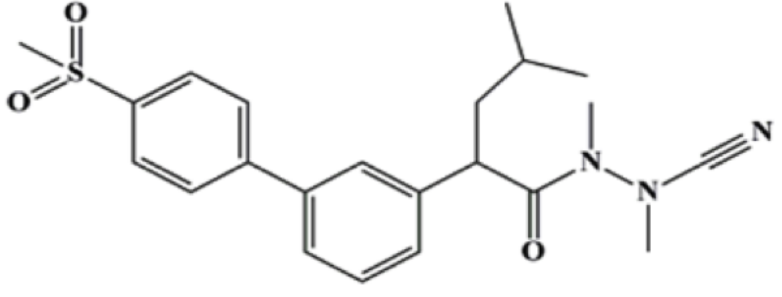

CKI-F